

Article

The Impacts of Regime Shift in Summer Arctic Oscillation on Precipitation in East Asia

Xuxin Zou ^{1,2}, Li Yan ^{1,2,*}, Jianjun Xu ^{1,2} and Shaojun Zheng ¹ 

¹ Laboratory for Coastal Ocean Variation and Disaster Prediction, South China Sea Institute of Marine Meteorology, College of Ocean and Meteorology, Guangdong Ocean University, Zhanjiang 524088, China; 2112102006@stu.gdou.edu.cn (X.Z.); jxu@gdou.edu.cn (J.X.); zhengsj@gdou.edu.cn (S.Z.)

² Shenzhen Institute of Guangdong Ocean University, Shenzhen 518120, China

* Correspondence: yanli@gdou.edu.cn

Abstract: Using multiple observational and reanalysis data, this paper investigates the impact of the interdecadal shift in summer Arctic Oscillation (AO) on precipitation in East Asia, by removing ENSO influences. The results indicate that the lower-layer activity center of summer AO in Atlantic shifted eastward after the mid-1980s. This regime shift of summer AO has a significant impact on precipitation in East Asia. Before the mid-1980s, the key regions in which precipitation was affected by AO in East Asia were northern East Asia and Northeastern China and adjacent regions. After the mid-1980s, the key regions in which precipitation was affected by AO in East Asia were central Inner Mongolia and Southern China. The mechanism of precipitation changes can be attributed to changes in atmospheric circulation and water vapor transport related to AO changes. After the mid-1980s, the influence of AO on geopotential height over northern East Asia weakened; meanwhile, the impact of AO on geopotential height over China increased. Consistent with the changes in atmospheric circulation, water vapor transport in East Asia also underwent interdecadal changes before and after the mid-1980s. The differences in atmospheric circulation and water vapor transport in East Asia can be traced back to the North Atlantic. Before the mid-1980s, wave activity flux related to summer AO tended to propagate in high latitudes and subtropics; after the mid-1980s, the wave activity flux changed in its subtropical path and propagated eastward from the North Atlantic through the Middle East to China, significantly affecting the summer precipitation in China.



Citation: Zou, X.; Yan, L.; Xu, J.; Zheng, S. The Impacts of Regime Shift in Summer Arctic Oscillation on Precipitation in East Asia. *Atmosphere* **2024**, *15*, 283. <https://doi.org/10.3390/atmos15030283>

Academic Editors: John Walsh and Christof Lüpkes

Received: 16 December 2023

Revised: 3 February 2024

Accepted: 23 February 2024

Published: 26 February 2024



Copyright: © 2024 by the authors. Licensee MDPI, Basel, Switzerland. This article is an open access article distributed under the terms and conditions of the Creative Commons Attribution (CC BY) license (<https://creativecommons.org/licenses/by/4.0/>).

Keywords: Arctic Oscillation; East Asia; summer precipitation; regime shift; water vapor transport; wave activity flux

1. Introduction

The Arctic Oscillation/North Atlantic Oscillation (AO/NAO) is the most important climate mode in the high-latitude regions of the Northern Hemisphere [1–4], with significant impacts on the Northern Hemisphere and regional climate variations [5–21]. The climate impacts of AO/NAO on the Eurasian continent are particularly pronounced. In recent decades, despite global warming, the much colder winters in mid-latitudes of Eurasia compared to the average have been associated with the negative phase of AO/NAO [22–24]. Zuo et al. [17] reported that the significant intra-seasonal zonal migration of AO/NAO in the center of the Azores led to different impacts of AO on temperature anomalies in early, mid, and late winter over Southern China from 1979 to 2011. Specifically, a weak positive relationship occurred in December, while a significant negative relationship occurred in January and February. It has been suggested that AO was at least partially related to the frequent and prolonged snowstorms in Central and Southern China in January 2008 [25]. In addition, accompanied by the obvious changes in the southern branch of the westerly jet stream to the south of the Tibetan Plateau, AO has exerted an important influence on large-scale winter precipitation events in China through its control of the water vapor

supply and weather activities [26–28]. The out-of-phase pattern of summer precipitation in the Yangtze River Basin and Southeastern China is related to the March NAO, while the out-of-phase pattern of summer precipitation in Northern China and the Yangtze River Basin is related to the January NAO [29]. Gong and Wang [30] and Xu et al. [31] revealed the in-phase relationship between the winter NAO and precipitation anomalies in Southwestern China. The Asian summer (e.g., [7,32]) and winter monsoon systems (e.g., [6,9,33]) are both affected by AO/NAO variations. A previous study found that the spatial structure of the North Pacific center of the spring AO is crucial for its impact on ENSO in the following winter [34]. In recent decades, global warming and the regional Arctic warming have been influenced by the combined effects of the Arctic Oscillation, the North Atlantic Oscillation, the Atlantic Multidecadal Oscillation, and the Pacific Decadal Oscillation [35,36]. Global warming and the regional Arctic warming are key drivers of the accelerated decline in summer Arctic sea ice [35,36]. The AO and NAO associated with adiabatic warming and humidification anomalies in the lower troposphere resulting from subsidence may exacerbate sea ice loss [37].

AO is significant in all seasons and strongest in winter. Previous studies have reported that the impact of AO on regional climates may be unstable during its strongest season (i.e., boreal winter) [18,38–45]. For instance, Li et al. [40] revealed that the relationship between AO and ENSO strengthened after the mid-1990s. Huang et al. [41] demonstrated that the connection between AO and the Siberian High was not stable in winter. In the past few decades, the relationship between the winter AO and the East Asian winter monsoon index has also undergone prominent interdecadal changes, and the relationship between the two has strengthened since 1983 [39]. Gong et al. [45] found that the winter AO undergoes interdecadal changes, and its impact on the East Asian surface air temperature (SAT) varies accordingly. Before the mid-1980s, the winter AO had a weak impact on the East Asian SAT and subsequently the impact increased.

Summer precipitation is often an important factor in determining the annual yields of crops [46,47]. In summer, AO is also likely to undergo interdecadal changes and have different impacts on summer precipitation in East Asia. Based on this issue, we explored the interdecadal variation in summer AO variability, as well as the relationship and the influencing mechanism between the summer AO and East Asian precipitation during different sub-periods. The remainder of this article is arranged as follows. Section 2 introduces the data and methods. Section 3 investigates the impact of the summer AO on precipitation in East Asia for different sub-periods. Section 4 further analyzes the corresponding mechanisms. A summary and discussion is provided in Section 5.

2. Data and Methods

2.1. Data

This study used two sets of atmospheric circulation data. One comprised the monthly global data from the National Centers for Environmental Prediction–National Center for Atmospheric Research (NCEP-NCAR) reanalysis (NCEP1; [48]), with a horizontal resolution of $2.5^\circ \times 2.5^\circ$, spanning from 1948 to 2021. We examined the sea level pressure (SLP), 850 and 200 hPa geopotential height fields (Z850 and Z200, respectively), zonal and meridional wind, and specific humidity. To verify the robustness of the results, we also calculated values based on another dataset for comparison, i.e., the Twentieth Century Reanalysis, version 3 (20CRv3; [49]). The 20CRv3 dataset has a $1^\circ \times 1^\circ$ horizontal resolution, spanning from 1851 to 2015.

Two sets of precipitation data were used in this study. One comprised the monthly land precipitation dataset from the GPCC [50], i.e., the Global Precipitation Climate Centre, with a spatial resolution of $1^\circ \times 1^\circ$. The research period of the GPCC data was selected covering 1948 to 2021, with the 1948–2016 data from the v2018 version and the 2017–2021 data from the first guess version. For these GPCC data, in the East Asia region, a total number of 4284 rain gauges are utilized, averaged from 1948 to 1984; a total number of 2984 rain gauges are utilized, averaged from 1985 to 2016. The other precipitation

dataset was obtained from the Physical Sciences Laboratory (PSL; [51]) in the University of Delaware. The time period for this precipitation dataset is from 1900 to 2017, with a horizontal resolution of $0.5^\circ \times 0.5^\circ$.

Considering that NCEP1 and GPCC cover a relatively recent period of time and the GPCC precipitation dataset is widely used, this article mainly reports the results based on the NCEP1 data and GPCC precipitation dataset.

We also used the monthly Extended Reconstructed Sea Surface Temperature version 5 (ERSSTv5, [52]) dataset, with a horizontal resolution of $2^\circ \times 2^\circ$.

2.2. Methods

This study focused on the interannual variability of AO under the background of interdecadal changes. The seasonality cycles were removed first in the data, and then the linear trends in all datasets were removed. Then, we applied a 3–120-month bandpass filter to all datasets.

Using empirical orthogonal function (EOF; [53]) decomposition, the summertime AO pattern is defined as the first EOF mode of the Z850 anomalies north of 20° N [3] during 1948–2021. The corresponding time series (TSs) of EOF1 represents the summer AO index. Here, the summer represents June, July, and August (JJA).

This study explains the mechanism of AO affecting precipitation in East Asia from three aspects: the geopotential height, water vapor transport, and the wave activity flux.

The atmospheric wave flux displays the propagation of waves in the atmosphere. This article presents the fluctuation changes in wave activities related to summertime AO during different periods. The expression for wave activity flux (W) is as follows, based on Takaya and Nakamura [54]:

$$W = \frac{p \cos \varphi}{2|\mathbf{U}|} \left(\frac{U}{a^2 \cos^2 \varphi} \left[\left(\frac{\partial \psi'}{\partial \lambda} \right)^2 - \psi' \frac{\partial^2 \psi'}{\partial \lambda^2} \right] + \frac{V}{a^2 \cos \varphi} \left[\frac{\partial \psi'}{\partial \lambda} \frac{\partial \psi'}{\partial \varphi} - \psi' \frac{\partial^2 \psi'}{\partial \lambda \partial \varphi} \right] \right. \\ \left. \frac{U}{a^2 \cos \varphi} \left[\frac{\partial \psi'}{\partial \lambda} \frac{\partial \psi'}{\partial \varphi} - \psi' \frac{\partial^2 \psi'}{\partial \lambda \partial \varphi} \right] + \frac{V}{a^2} \left[\left(\frac{\partial \psi'}{\partial \varphi} \right)^2 - \psi' \frac{\partial^2 \psi'}{\partial \varphi^2} \right] \right) \quad (1)$$

where ψ' represents the stream function anomalies, a denotes the radius of the Earth, U and V , respectively, are the zonal and meridional components of the basic flow, $|\mathbf{U}|$ is the climatological mean wind speed, p is the pressure divided by 1000 hPa, and (φ, λ) indicates the latitude and longitude, respectively.

The El Niño Southern Oscillation (ENSO) also has an impact on precipitation in East Asia [55–57]. To investigate the impact of AO on summer precipitation in East Asia by removing the influence of ENSO, a partial correlation method was used [58]. The partial correlation is expressed as follows [58]:

$$R_{ab,c} = \frac{R_{ab} - R_{ac}R_{bc}}{\sqrt{(1 - R_{ac}^2)(1 - R_{bc}^2)}} \quad (2)$$

where R_{ab} represents the correlation coefficient between variable a and variable b , while $R_{ab,c}$ is the partial correlation between variable a and variable b after the influence of variable c is excluded. The ENSO signal is expressed by the monthly Nino 3.4 sea surface temperature (SST), which is the average of the SST anomalies in the region (5° N– 5° S, 170° W– 120° W).

3. Impacts of AO on Precipitation in East Asia before and after Mid-1980s

3.1. Interdecadal Changes in AO in the North Atlantic

AO has undergone significant interdecadal changes in the North Atlantic Ocean. A previous study showed that AO/NAO strengthened during winter in the mid-1980s [19]. Our results also indicate that, during summer, AO/NAO strengthened in the mid-1980s (Figure 1). In terms of sea level pressure (SLP), the relationship between AO and SLP in the Atlantic Ocean and the whole Eurasian continent changed in the mid-1980s. Particularly in the Atlantic Ocean and the neighboring Europe, before the mid-1980s, the positive

correlation between AO and SLP was mainly confined to Western Europe (Figure 1a). After the mid-1980s, the correlation between AO and SLP in the North Atlantic, Western Europe, and Scandinavia significantly increased (Figure 1b). Such a regime shift of the SLP is a manifestation of the strengthening of AO/NAO. After removing the influence of ENSO, the results are consistent. With the interdecadal changes in AO, its impact on precipitation in Europe also changes, which is a local effect.

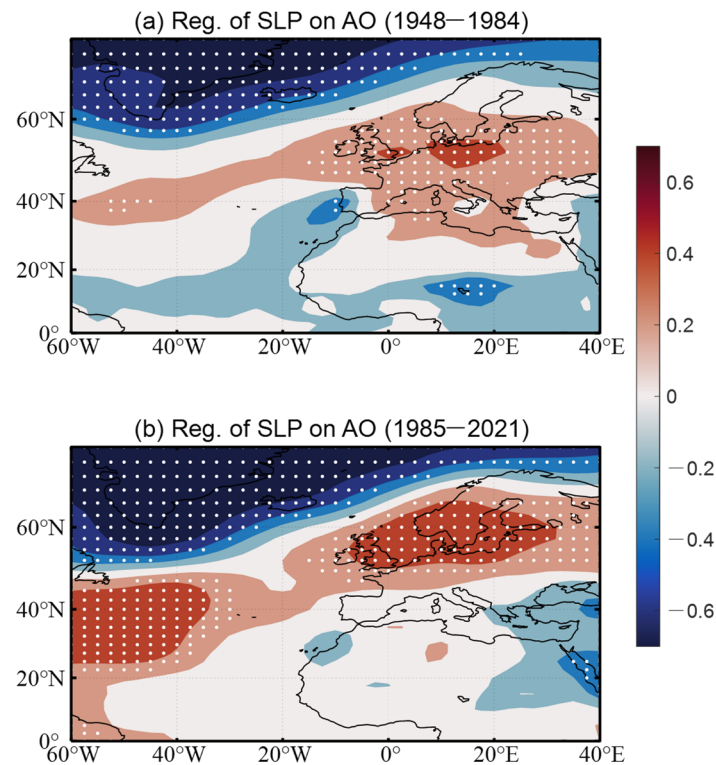


Figure 1. Regression of the JJA SLP on the AO index (a) from 1948 to 1984 and (b) from 1985 to 2021 over the North Atlantic. All the indices have been normalized. The dotted areas indicate that the correlations are significant at a 90% confidence level.

3.2. Impacts of AO on Precipitation in East Asia

This study primarily discusses the impact of AO on precipitation in East Asia during different sub-periods and the mechanisms. Especially in China, which is under the control of the East Asian summer monsoon, flood season disaster events are often prone to occur in summer. Considering that ENSO also has an impact on precipitation in Eurasia [59–62], this study compares the relationship between summertime AO and East Asian precipitation for different sub-periods, with the influence of ENSO excluded (Figure 2). Considering that precipitation is influenced by multiple factors and is complex, previous studies on precipitation (e.g., [44,61,63,64]) have used a confidence level of 80% to 90%. Thus, the use of 90% as the confidence level for precipitation in this study is also regarded as significant and credible. Before the mid-1980s (Figure 2a), significant negative correlations were located in northern East Asia; significant positive correlations were located in the northeast of China and adjacent regions. After the mid-1980s (Figure 2b), there was a significant change in the key regions. The negative correlation in northern East Asia disappeared, and the positive correlation around Northeastern China shifted northwestward to the north of 55° N. At the same time, two key regions with a positive correlation emerged, with one appearing in central Inner Mongolia and adjacent areas and the other in Southern China (Figure 2b).

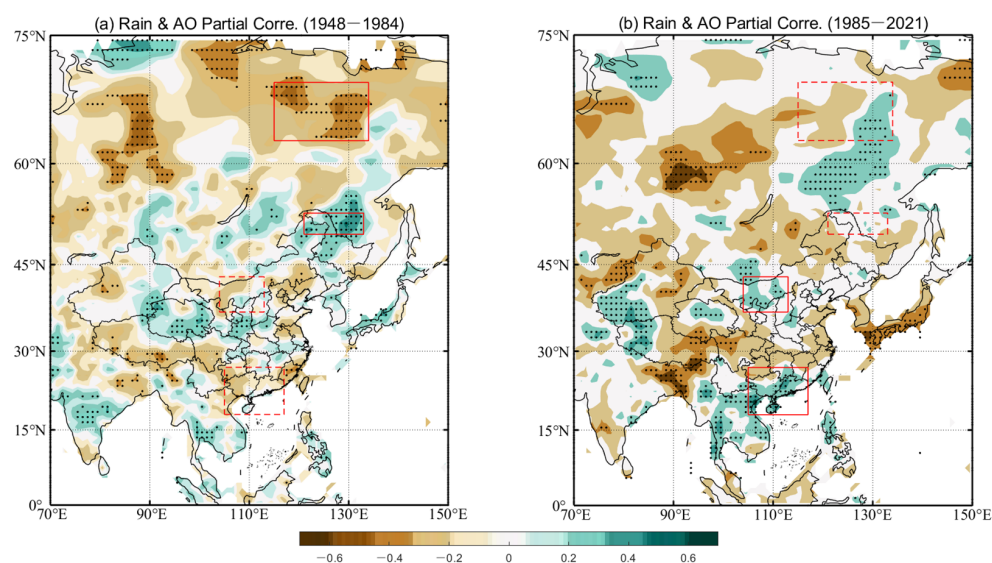


Figure 2. Partial correlations (by removing the influence of ENSO) between JJA precipitation and the JJA AO index (a) from 1948 to 1984 and (b) from 1985 to 2021. All the indices have been normalized. The dotted areas indicate that the partial correlations pass the confidence test at a 90% confidence level. The red boxes represent the four key precipitation areas selected.

To quantitatively identify the contributions of AO to the precipitation anomalies in East Asia, four key precipitation regions were selected based on the significant correlation areas in Figure 2. The key regions are northern East Asia (NEA, 115° E–134° E, 63° N–70° N), Northeastern China and adjacent regions (NECA, 121° E–133° E, 50° N–53° N), central Inner Mongolia and adjacent regions (CIMA, 104° E–113° E, 37° N–43° N), and Southern China (SC, 105° E–117° E, 18° N–27° N). The area-averaged precipitation anomalies in these four chosen regions were calculated to construct corresponding precipitation indices.

Figure 3 displays the scatter diagrams of the AO index versus precipitation in the above four key regions over the two sub-periods. Before the mid-1980s, the AO mode significantly influenced the summer precipitation in northern East Asia (Figure 3a) and Northeastern China and adjacent regions (Figure 3c). Among them, the AO index was negatively correlated with the NEA_Rain index (correlation = -0.42 , Figure 3a) and the AO index was positively correlated with the NECA_Rain index (correlation = 0.27 , Figure 3c), both significant at a 90% confidence level. There were nine (eight) rainy (drought) summer events in northern East Asia (Figure 3a) before the mid-1980s, among which four (three) years were influenced by AO. Accordingly, AO contributed to 44% (38%) of the rainy (drought) summer events in northern East Asia. Similarly, there were five (seven) rainy (drought) summer events in Northeastern China and adjacent regions, with one (three) year dominated by AO (Figure 3c). Therefore, AO accounted for about 20% (43%) of the rainy (drought) summer events in Northeastern China and adjacent regions.

After the mid-1980s, the AO mode no longer significantly affected the precipitation in northern East Asia and Northeastern China (Figure 3b,d), but it could significantly influence the summer precipitation in central Inner Mongolia and its adjacent regions, as well as in Southern China (Figure 3f,h). The AO index was positively correlated with the CIMA_Rain index (correlation = 0.29 , Figure 3f) and the AO index was positively correlated with the SC_Rain index (correlation = 0.27 , Figure 3h), both significant at a 90% confidence level. During 1985–2021, there were seven (six) summer rainy (drought) events in central Inner Mongolia, with three (two) years affected by AO, and seven (six) summer rainy (drought) events in Southern China, with two (three) years affected by AO. The contribution rates of AO to summer rainy (drought) events in central Inner Mongolia and Southern China were 43% (33%) and 29% (50%), respectively.

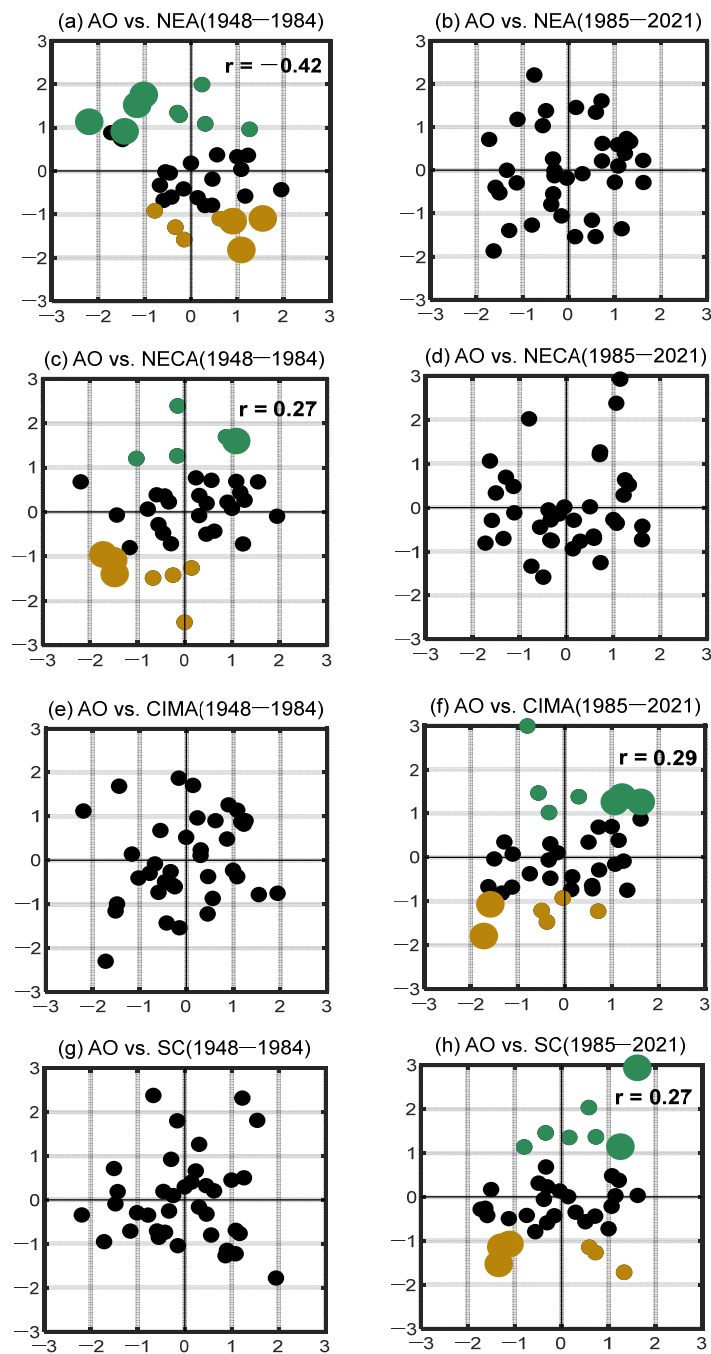


Figure 3. Scatterplot of AO index (x axis) versus (a) NEA_Rain, (c) NECA_Rain, (e) CIMA_Rain, and (g) SC_Rain (y axis) before the mid-1980s. (b,d,f,h) as in (a,c,e,g), but for the period after the mid-1980s. The green (brown) dots represent rainy (drought) summer events with normalized values greater than (less than) 0.90 (−0.90). The bolded green (brown) dots indicate the rainy (drought) summer events contributed by AO (i.e., the absolute value of the standardized AO index exceeds 0.90). The bolded r indicates that the correlation is statistically significant at a 90% confidence level.

4. The Mechanism of AO Affecting Summer Precipitation in East Asia

4.1. Geopotential Height

We first examined the geopotential height at the low-layer atmosphere (850 hPa). In the North Atlantic and neighboring regions, compared to before 1985 (Figure 4a), the positive center of the wave train modes related to AO over Western Europe had a noticeably larger spatial range and stronger amplitude after 1985 (Figure 4b). This center also moved

northward and extended eastward after 1985. In this region, the variation in the 850 hPa geopotential height field (Figure 4) was consistent with the variation in the sea level pressure field (Figure 1). These results indicate that the interdecadal variability of AO is associated with changes in its lower-layer atmospheric spatial pattern over the North Atlantic and adjacent regions. The manifestation of this change in summer involves an obvious eastward shift and increased amplitude, consistent with the winter situation [17]. Therefore, the different teleconnection effects of AO on the downstream regional climate are largely attributed to the significant zonal migration of the lower-layer AO activity center over the North Atlantic sector.

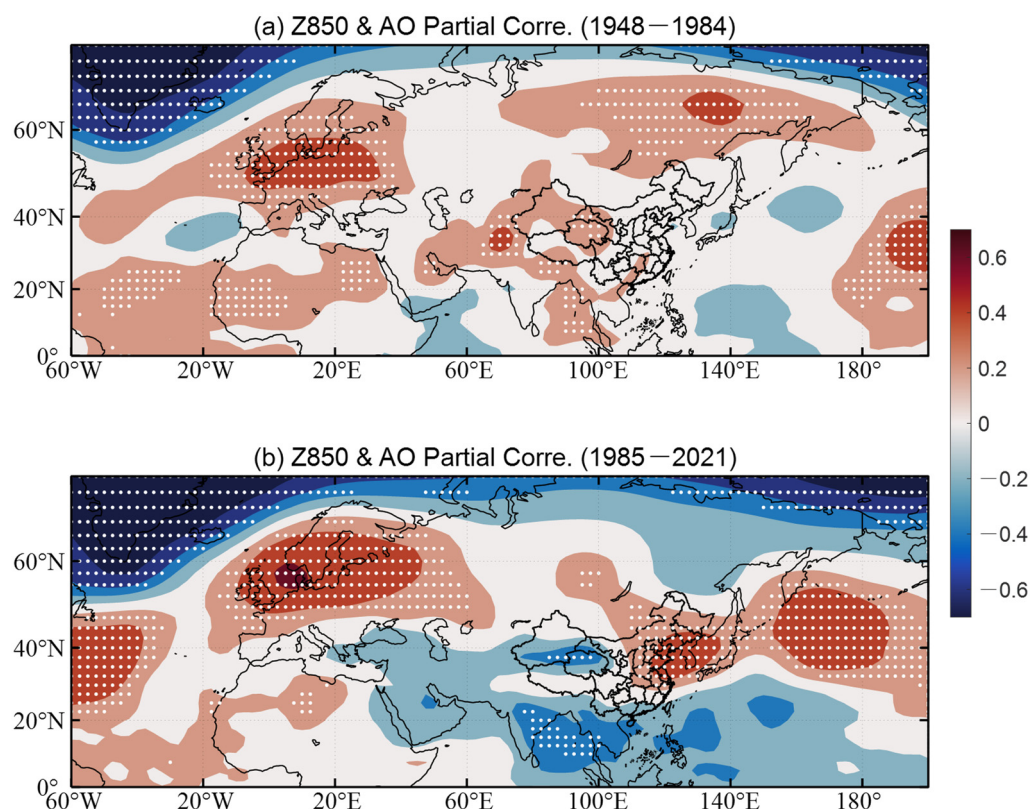


Figure 4. Partial correlations (by removing the influence of ENSO) between the JJA Z850 and the JJA AO index (a) from 1948 to 1984 and (b) from 1985 to 2021. All the indices have been normalized. The dotted areas indicate that the partial correlations pass the confidence test at a 90% confidence level.

In East Asia, the spatial pattern of the low-level atmospheric geopotential height related to AO has also undergone significant changes since the mid-1980s. Before the mid-1980s, the 850 hPa geopotential height in northern East Asia was positively correlated with AO (Figure 4a), and the positively correlated area was distributed in an east–west zonal pattern. The correlation between AO and the 850 hPa geopotential height field in China was weak and not significant during this period. After the mid-1980s (Figure 4b), the influence of AO on the 850 hPa geopotential height in northern East Asia weakened. The impact of AO on the 850 hPa geopotential height in the China region increased.

The influence of AO on the potential height field of the upper atmosphere (Figure 5) also showed interdecadal variations before and after 1985, especially in East Asia. Before the mid-1980s (Figure 5a), there was a significant positive correlation between the 200 hPa geopotential height and AO in northern East Asia; there were weak negative correlations in Northern China, Mongolia, and the vicinity of Sakhalin Island, and a weak positive correlation in Southern China. After the mid-1980s (Figure 5b), the influence of AO on the 200 hPa geopotential height in northern East Asia weakened, while the impact of AO on the 200 hPa geopotential height in China increased. Among them, Northern China

is a significantly positively correlated region, while Southern China is a significantly negatively correlated region. The results obtained from the 20CRv3 data are consistent with those obtained from the NCEP1 (Figures 4 and 5) data, both in the lower- and upper-level atmosphere.

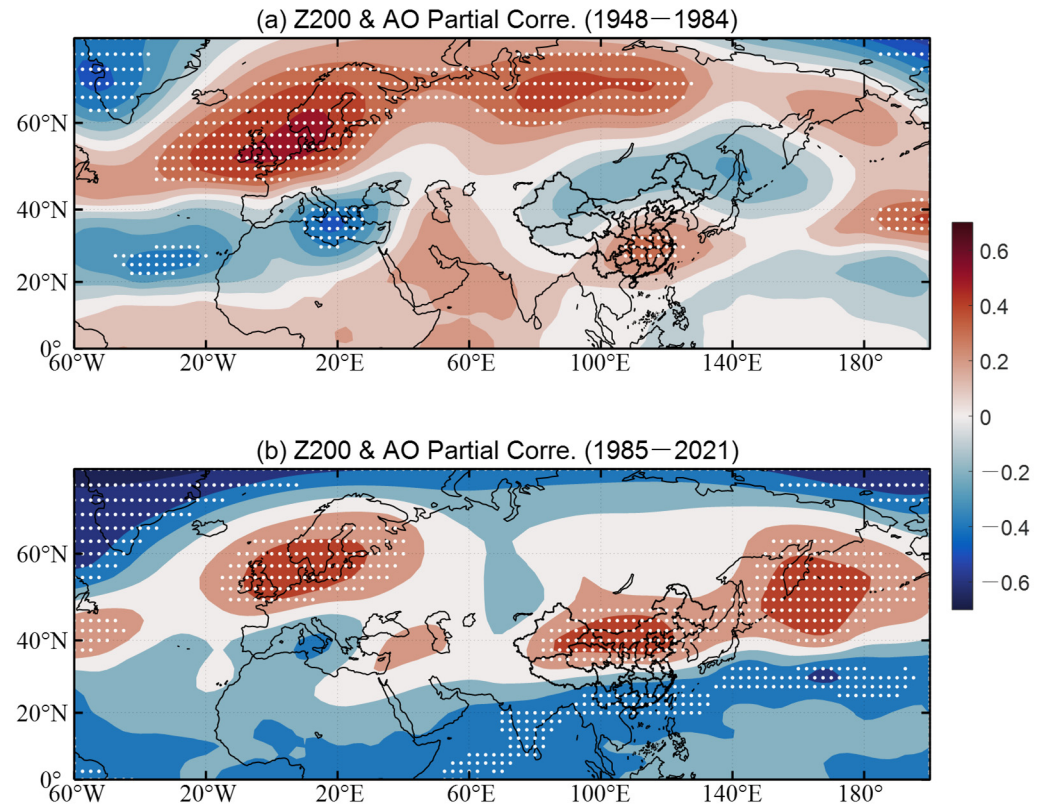


Figure 5. As in Figure 4, but for the partial correlations (by removing the influence of ENSO) between the JJA Z200 and the JJA AO index.

These results indicate that, around 1985, atmospheric circulation anomalies related to AO exhibited different spatial patterns in the mid and high latitudes of Eurasia, transporting the non-stationary AO effects eastward to East Asia through zonal wave trains in the mid to high latitudes, further leading to changes in the relationship between summer AO and East Asian summer precipitation anomalies.

4.2. Water Vapor Transport

Water vapor is an important factor leading to rainfall. Water vapor is mainly distributed over the lower troposphere; the low-level anomalous cyclonic (anticyclonic) circulation related to summer AO corresponds to the anomalous convergence (divergence) of moisture over Eurasia (Figure 6). The convergence (divergence) of the water vapor is usually associated with an increase (decrease) in rainfall. The patterns of the 850 hPa moisture flux (Figure 6) explain the precipitation patterns (Figure 2). The following analysis of water vapor flux is for the situation in which AO is in the positive phase; for negative AO years, the situation is the opposite.

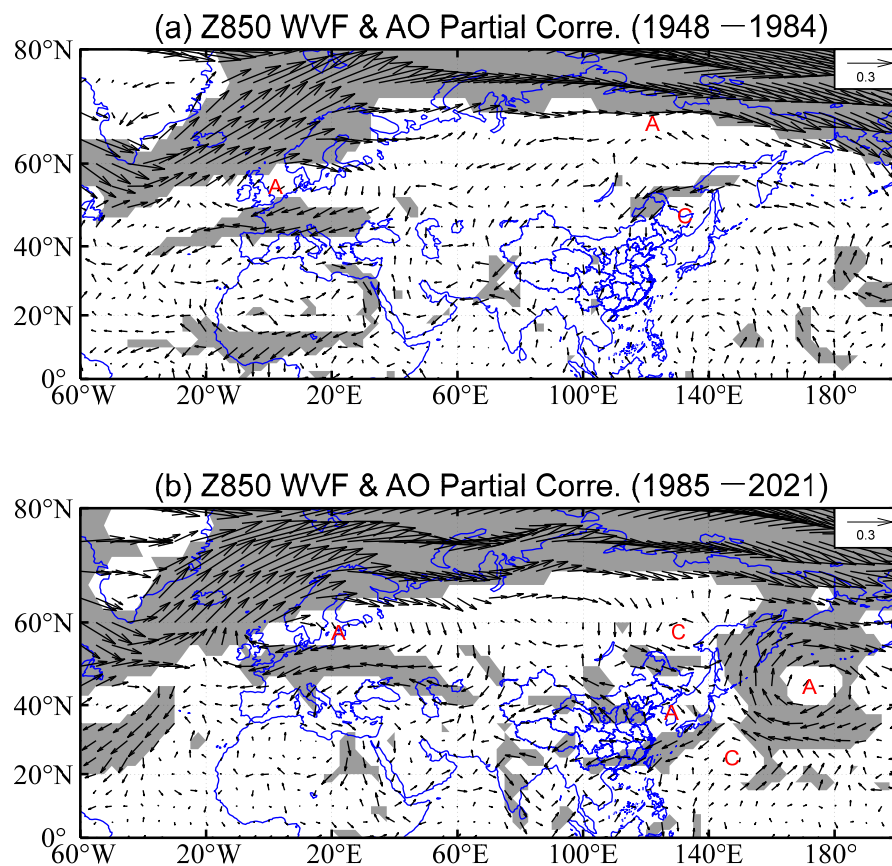


Figure 6. Partial correlations (by removing the influence of ENSO) between the JJA water vapor flux at 850 hPa and the JJA AO index (a) from 1948 to 1984 and (b) from 1985 to 2021. All the indices have been normalized. The shadings indicate that the partial correlations are statistically significant at a 90% confidence level. The blue lines represent the national boundaries and provincial boundaries of China and the coastlines of continents. The letter A stands for water vapor divergence and the letter C stands for water vapor convergence.

Before the mid-1980s, for positive AO years, a moisture divergence center emerged over northern East Asia (Figure 6a), which explains the negative precipitation anomaly in northern East Asia during this period (Figure 2a). Additionally, a water vapor convergence center emerged near Northeastern China (Figure 6a), and the easterly airflow in the northern part of the cyclone enhanced the water vapor transport from the Northwest Pacific to Northeastern China, resulting in an increase in precipitation in Northeastern China and adjacent areas (Figure 2a).

After the mid-1980s, for positive AO years, the divergence center in northern East Asia disappeared (Figure 6b). Therefore, the negative precipitation anomaly in northern East Asia disappeared after the mid-1980s (Figure 2b). At the same time, due to the convergence center near Northeastern China moving approximately 10° northward (Figure 6b), the area of positive anomalous precipitation in Northeastern China also moved northward (Figure 2b). In addition, a water vapor divergence center emerged on the Korean Peninsula (Figure 6b), and a large amount of eastward water vapor was continuously transported to the eastern areas of China. These water vapor centers are divided into two paths (Figure 6b): one enters central Inner Mongolia and adjacent areas, causing positive precipitation anomalies there; and the other is transported southward to Southern China, resulting in abundant summer rainfall there (Figure 2b). In addition, water vapor transport into Inner Mongolia can extend further inland and be transported to northern Qinghai Province and western Xinjiang Province (Figure 6b). Hence, positive precipitation anomalies can also be observed in some regions of Northwestern China (Figure 2b).

Figure 7 further illustrates the vertically integrated water vapor flux from the surface to 300 hPa, which is consistent with the low-level water vapor flux pattern in Figure 6. However, the intensity of the integrated water vapor flux is stronger, especially for the second sub-period (Figure 7b). These results indicate that water vapor transport anomalies related to AO exhibit different spatial distribution characteristics in the Eurasian region before and after the mid-1980s, leading to significant interdecadal changes in the relationship between AO and summer precipitation anomalies in East Asia.

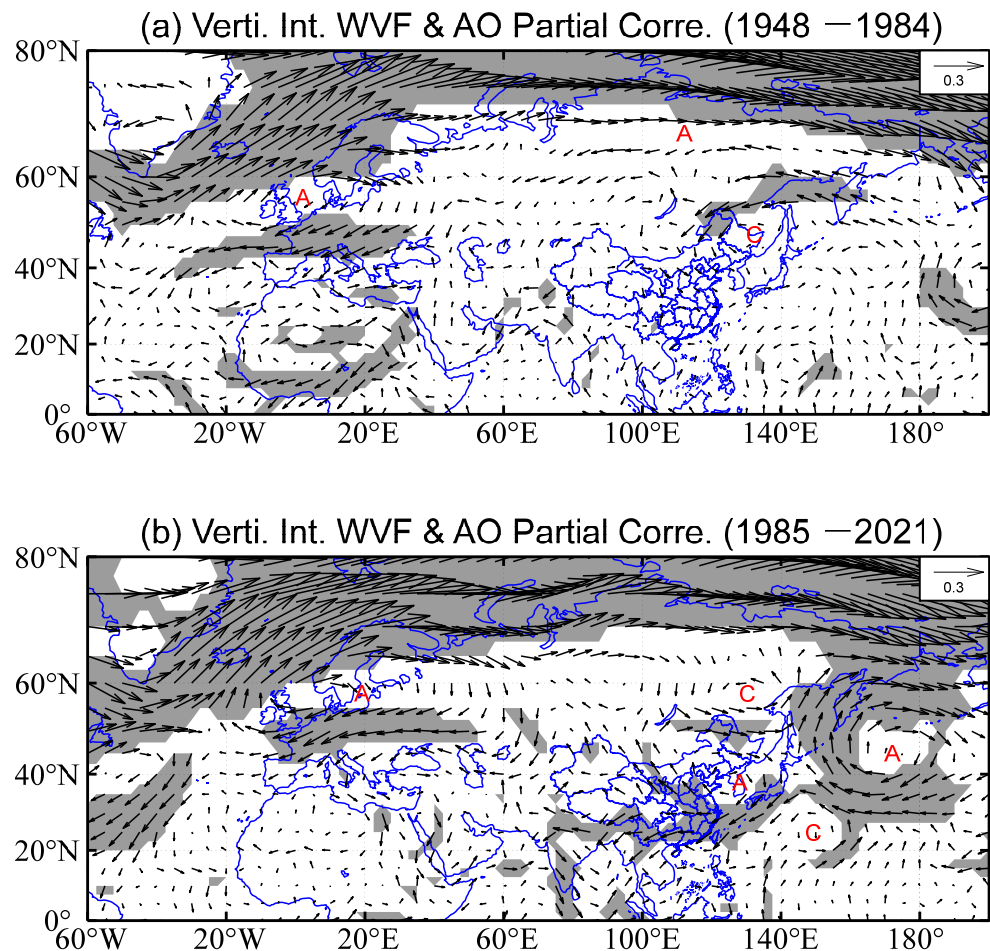


Figure 7. As in Figure 6, but for the partial correlations (by removing the influence of ENSO) between the JJA vertically integrated water vapor flux (From the surface to 300 hPa) and the JJA AO index.

From the perspective of the water vapor budget, Figure 8 displays the divergence of the vertically integrated water vapor flux. Focusing on the East Asian region, before the mid-1980s (Figure 8a), for positive AO years, a divergence center of vertically integrated water vapor flux appeared over northern East Asia, corresponding to the negative precipitation anomaly in northern East Asia before the mid-1980s (Figure 2a). Additionally, a convergence center of vertically integrated water vapor flux appeared near Northeastern China, corresponding to the positive precipitation anomaly in Northeastern China and adjacent areas (Figure 2a). Meanwhile, after the mid-1980s (Figure 8b), for positive AO years, the divergence center and the related negative precipitation anomaly (Figure 2b) in northern East Asia disappeared. At the same time, the convergence center near Northeastern China and the related positive precipitation anomaly (Figure 2b) moved northward. In addition, convergences emerged in central Inner Mongolia and adjacent areas, agreeing well with the positive precipitation anomalies there (Figure 2b), and convergences also emerged in Southern China, agreeing well with the plentiful rainfall there (Figure 2b).

These results based on the divergence of the vertically integrated water vapor flux are consistent with those from the lower-level and integrated water vapor flux.

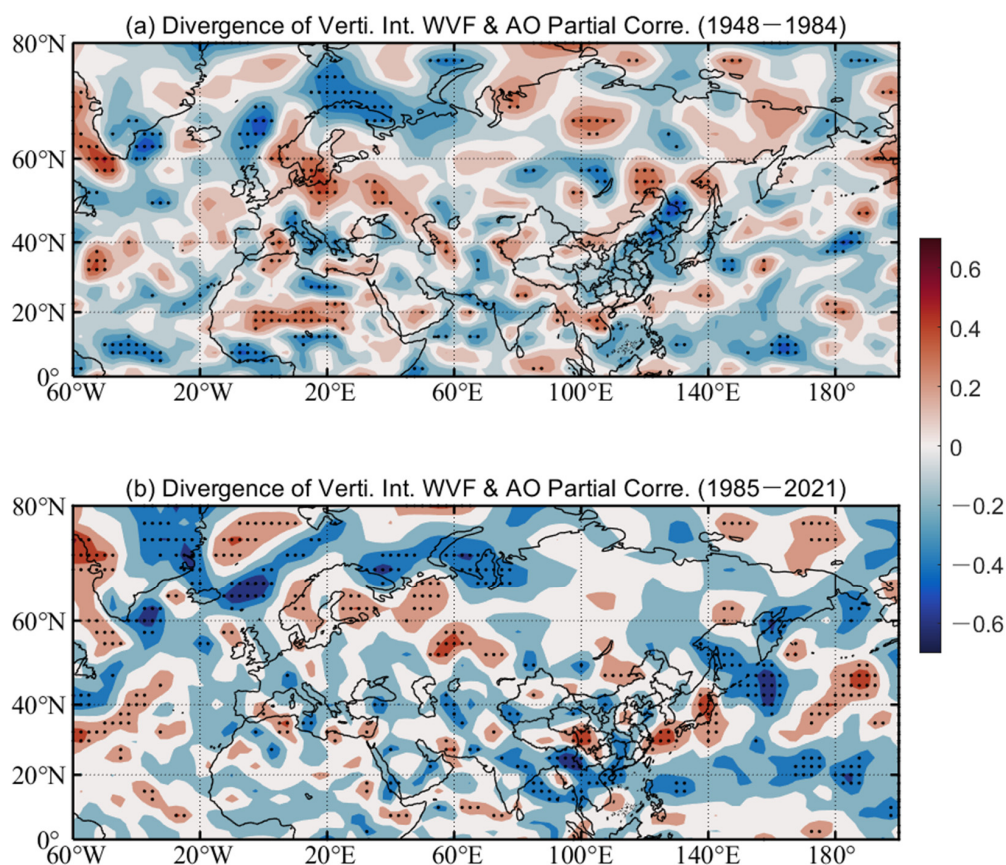


Figure 8. Partial correlations (by removing the influence of ENSO) between the JJA divergence of vertically integrated water vapor flux and the JJA AO index (a) from 1948 to 1984 and (b) from 1985 to 2021. All the indices have been normalized.

4.3. Wave Activity Flux

Regarding large-scale circulations in mid–high latitudes, Rossby waves are the main mechanism for their formation and maintenance. A previous study suggested that the persistent anomalies in atmospheric circulation are clearly connected with planetary wave activity [65]. The propagation of quasi-steady planetary waves involves wave energy dispersion, and its propagation and evolution are dynamic processes closely related to the interaction between waves and currents. Due to the mid-latitude westerlies acting as Rossby wave guides [66], wave energy propagates eastward along the westerly belt to East Asia. This process can be accurately represented by examining the wave activity flux. Takaya and Nakamura [54,67] proposed the concept of the TN wave activity flux and demonstrated that the wave activity flux is parallel to the local group velocity of the Rossby wave, which can be used to describe the propagation of atmospheric wave trains. Many studies have shown that atmospheric wave trains play an important role in influencing temperature and precipitation patterns. For instance, a study [68] found that the atmospheric wave trains across the mid–high latitudes of Eurasia made a considerable contribution to the persistent heavy rainfall events in Southern China during the first rainy season (April–June). It is reported that the simultaneous summer heat waves over Northern China and Eastern Europe are caused by atmospheric teleconnections over the Eurasian continent [69]. The springtime atmospheric wave activity can lead to temperature anomalies over Eurasia through wind-induced horizontal temperature advection and cause precipitation anomalies by regulating the upper and lower tropospheric divergence [70].

The summer AO/NAO can significantly modulate the Asian summer climate variability via Rossby wave trains (e.g., [13,71–78]). These Rossby waves associated with AO/NAO include the circumglobal teleconnection pattern (CGT) or the Silk Road pattern (SRP) (e.g., [66,72,79–82]). The SRP is an important component of the CGT and can be considered as the CGT on the Eurasian continent (e.g., [72,82]).

The SRP or CGT, modulated by AO (e.g., [74,76,83–85]), not only influences the summer precipitation in Europe [72], India [72,86], Central Asia [87,88], etc., but also extends eastward to further influence the summer precipitation in East Asia (e.g., [80,85]), including China (e.g., [81,89]). For example, Jin and Guan [81] found that the CGT can act as a bridge in the relationship between AO and the Hetao–Yangtze rainfall seesaw in China. During the positive AO phase, due to the impact of the CGT, the circulations over Hetao and the middle and lower reaches of the Yangtze River (MLRYR) were disturbed, and consequently the north–south rainfall seesaw was generated. Hong et al. [85] indicated that NAO was closely associated with the SRP, and Du et al. [89] reported that the circulation anomalies associated with extreme drought in Northern China were related to the eastward shift of the negative phase of the summer AO/NAO.

According to Takaya and Nakamura [54], Figure 9 shows the spatial patterns of the 200 hPa wave activity flux associated with the summertime AO in two sub-periods. Before the mid-1980s (Figure 9a), for positive AO years, the wave activity flux is strong in the North Atlantic region. The AO activity center over the North Atlantic seems to favor a branch of anomalous wave activity flux that propagates eastward into the Northern Eurasian continent and forms a wave train across the high latitudes of Eurasia, consistent with the wave train along the subpolar waveguide [66]. During this period, positive stream function anomalies dominated northern East Asia (Figure 9a), leading to negative precipitation anomalies in this region (Figure 2a). Meanwhile, for its subtropical branch, the Atlantic divergences as well as the Mediterranean convergence anomalies in the upper troposphere appeared as the Rossby wave source and excited the CGT in the subtropics (Figure 9a).

After the mid-1980s (Figure 9b), the AO-associated anomalous wave activity remained strong in the North Atlantic region, but the high-latitude wave train disappeared. At this time, the wave train's position on the Eurasian continent tended to be southward, and the subtropical path of the waves was significantly changed (Figure 9b). This wave train is accompanied by positive stream function anomalies over Europe and the Arabian Peninsula, as well as negative stream function anomalies over the Mediterranean and North Africa. They propagate from the North Atlantic through the Middle East into East Asia, forming a meridional dipole mode in the stream function in China, significantly affecting summer precipitation in China (Figure 2b). This subtropical propagation has been recognized in previous studies [28,32]. In the upper troposphere, anomalous divergences in the North Atlantic and anomalous convergences in the Mediterranean could also be observed (Figure 9b). The Atlantic divergences as well as the Mediterranean convergence anomalies also emerged as the Rossby wave source and excited the CGT, displaying the eastward propagation of the Rossby wave in the subtropics and becoming stronger in China (Figure 9b). In other words, the subtropical path of the wave train resembles the circumglobal teleconnection (CGT) pattern [72,81].

In short, the anomalous wave activity flux serves as a bridge connecting the AO and the Eurasian atmospheric circulation, propagating the AO signal from the North Atlantic eastward to Europe and East Asia, inducing local atmospheric circulation anomalies and further affecting the summer precipitation in these regions. The differences in the wave activity flux related to the summer AO between the two sub-periods may lead to interdecadal variations in the relationship between AO and summer precipitation in East Asia.

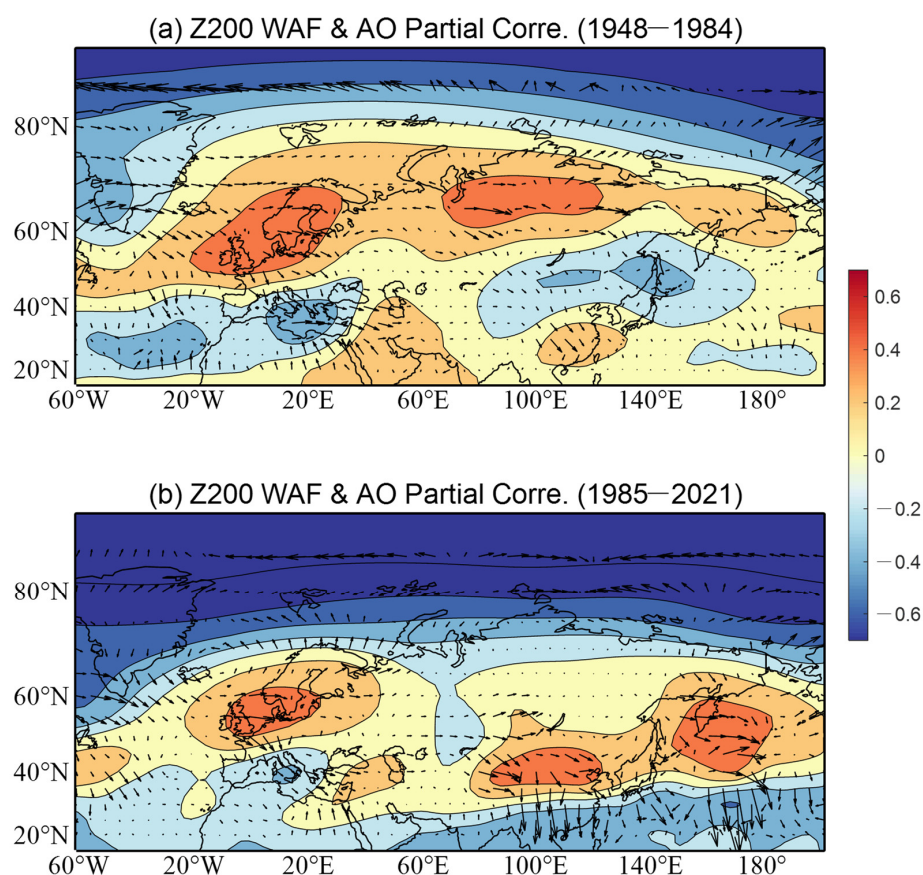


Figure 9. Partial correlations (by removing the influence of ENSO) between the JJA horizontal wave activity flux (vectors) and stream function (shading) at 200 hPa and the JJA AO index (a) from 1948 to 1984 and (b) from 1985 to 2021.

5. Summary and Discussion

This study investigated the relationship between the summer AO and East Asian rainfall in two sub-periods. The results indicate that the summer AO activity center in the lower atmosphere of the North Atlantic strengthened and moved eastward after the mid-1980s. With the interdecadal changes in the spatial pattern of the summer AO over the North Atlantic, the influence of AO on East Asian summer rainfall also exhibited different patterns before and after the mid-1980s. Before the mid-1980s, the key regions in which precipitation was affected by AO in East Asia were northern East Asia (NEA) and Northeastern China and adjacent regions (NECA). After the mid-1980s, the key regions in which precipitation was affected by AO in East Asia were central Inner Mongolia (CIMA) and Southern China (SC). Among these four key regions, AO has a negative correlation with rainfall in NEA, while AO has a positive correlation with rainfall in the NECA, CIMA, and SC regions. Further research reveals that, based on GPCC data, the contributions of the summer AO to rainy (drought) events in NEA, NECA, CIMA, and SC are 44% (38%), 20% (43%), 43% (33%), and 29% (50%), respectively. The results based on the PSL rainfall data are basically consistent with the GPCC data.

The interdecadal variation in the relationship between the summer AO and East Asian rainfall can be attributed to the eastward shift of the atmospheric low-level activity center of the summer AO in the North Atlantic. The changes in the spatial pattern of AO in the Atlantic have led to changes in the response pattern of the geopotential heights at mid to high latitudes in Eurasia. In East Asia, before the mid-1980s, there was a significant correlation between AO and rainfall in northern East Asia, and this significant correlation area was distributed in an east–west zonal band. The correlation between AO and the 850 hPa geopotential height in China was weak during 1948–1984. After the mid-1980s,

the influence of AO on the geopotential height in northern East Asia weakened, and the impact of AO on the geopotential height in China increased.

The spatial patterns of precipitation are closely related to the moisture conditions. Water vapor transport in East Asia also underwent interdecadal changes before and after the mid-1980s. Taking positive AO years for example, before the mid-1980s, NEA and NECA were, respectively, controlled by divergent and convergent water vapor flux, resulting in drought and rainy events, respectively. However, after the mid-1980s, the divergence center in NEA disappeared, while the convergence center in NECA moved northward by about 10° . Therefore, the negative precipitation anomalies in NEA disappeared and the positive precipitation anomalies in NECA moved northwestward during 1985–2021. Meanwhile, a moisture divergence center emerged over the Korean Peninsula, with a substantial amount of easterly water vapor continuously transported to the eastern areas of China and divided into two paths. Water vapor in one path influenced CIMA, leading to positive precipitation anomalies there, while water vapor in the other transported southward, providing abundant summer rainfall in SC. The situations for negative AO years are the opposite. The vertically integrated water vapor flux from the surface to 300 hPa and the divergence of vertically integrated water vapor flux also support these findings.

The differences in atmospheric circulation and water vapor transport can be traced back to the North Atlantic. Such changes in the summertime AO pattern can alter the wave activity flux over the Eurasian continent. The zonal wave train associated with AO can serve as a bridge to transport the distinct impacts of the summer AO eastward to East Asia. The Rossby wave train in the subtropics resembles the CGT or SRP pattern and propagates eastward. Before the mid-1980s, wave activity related to the summer AO propagating eastward at high latitudes to northern East Asia was stronger than that in the subtropical path. After the mid-1980s, the high-latitude wave train disappeared, while the wave train in the subtropical path changed and propagated eastward from the North Atlantic through the Middle East to China, significantly affecting the summer precipitation in China.

Although the AO is primarily generated by internal atmospheric dynamics [90], it may also be influenced by the lower-level sea surface temperature [12,91,92]. Some studies document that the reduction of Arctic sea ice can have distant impacts on the Eurasian climate by stimulating the propagation of Rossby waves [93–95]. Furthermore, global warming has led to frequent extreme precipitation events worldwide [96,97], and interdecadal changes in AO also occur under the background of global warming [98]. Thus, the impact of global warming on the interdecadal changes in AO, how Arctic sea ice affects extreme precipitation in East Asia, and the combined effects of AO and other factors on precipitation in East Asia are worth further exploration.

Author Contributions: Conceptualization, L.Y. and X.Z.; methodology, L.Y. and X.Z.; software, X.Z. and L.Y.; formal analysis, X.Z., L.Y., J.X. and S.Z.; data curation, S.Z. and X.Z.; writing—original draft preparation, X.Z. and L.Y.; writing—review and editing, L.Y. and J.X.; visualization, X.Z.; funding acquisition, L.Y., J.X. and S.Z. All authors have read and agreed to the published version of the manuscript.

Funding: This study was jointly supported by the Shenzhen Science and Technology Program (JCYJ20210324131810029), the National Natural Science Foundation of China (72293604 and 42130605), and the program for scientific research start-up funds of Guangdong Ocean University (R19061 and R18023).

Institutional Review Board Statement: Not applicable.

Informed Consent Statement: Not applicable.

Data Availability Statement: The NCEP1 dataset was downloaded from <https://www.esrl.noaa.gov/psd/data/gridded/data.ncep.reanalysis.pressure.html> (accessed on 24 March 2022). The 20CRv3 dataset was obtained from https://psl.noaa.gov/data/gridded/data.20thC_ReanV3.html (accessed on 12 October 2022). The GPCC precipitation dataset is available at <https://psl.noaa.gov/data/gridded/data.gpcc.html> (accessed on 19 May 2022). The monthly mean precipitation dataset from the University of Delaware, provided by the Physical Sciences Laboratory, can be found at <https://psl>.

noaa.gov/data/gridded/data.UDel_AirT_Precip.html (accessed on 24 December 2022). The ERSSTv5 dataset was obtained from <https://psl.noaa.gov/data/gridded/data.noaa.ersst.v5.html> (accessed on 17 June 2022). The datasets used in this study are publicly available online.

Acknowledgments: The authors would like to thank the editors and the anonymous reviewers.

Conflicts of Interest: The authors declare no conflicts of interest.

References

- Wallace, J.M.; Gutzler, D.S. Teleconnections in the Geopotential Height Field during the Northern Hemisphere Winter. *Mon. Weather Rev.* **1981**, *109*, 784–812. [[CrossRef](#)]
- Thompson, D.W.J.; Wallace, J.M. The Arctic oscillation signature in the wintertime geopotential height and temperature fields. *Geophys. Res. Lett.* **1998**, *25*, 1297–1300. [[CrossRef](#)]
- Thompson, D.W.J.; Wallace, J.M. Annular modes in the extratropical circulation. Part I: Month-to-month variability. *J. Clim.* **2000**, *13*, 1000–1016. [[CrossRef](#)]
- Li, J.; Wang, J.X.L. A modified zonal index and its physical sense. *Geophys. Res. Lett.* **2003**, *30*, 1632. [[CrossRef](#)]
- Hurrell, J.W. Decadal Trends in the North Atlantic Oscillation. *Science* **1995**, *269*, 676–679. [[CrossRef](#)] [[PubMed](#)]
- Gong, D.; Wang, S.; Zhu, J. East Asian Winter Monsoon and Arctic Oscillation. *Geophys. Res. Lett.* **2001**, *28*, 2073–2076. [[CrossRef](#)]
- Gong, D.; Ho, C.H. Arctic Oscillation signals in the East Asian summer monsoon. *J. Geophys. Res.* **2003**, *108*, 4066. [[CrossRef](#)]
- Hurrell, J.W.; Kushnir, Y.; Ottersen, G.; Visbeck, M. An overview of the North Atlantic Oscillation. *Geophys. Monogr. Ser.* **2003**, *134*, 1–35. [[CrossRef](#)]
- Jeong, J.H.; Ho, C.H. Changes in occurrence of cold surges over east Asia in association with Arctic Oscillation. *Geophys. Res. Lett.* **2005**, *32*, L14704. [[CrossRef](#)]
- Yan, H.; Wan, Y.; Cheng, J. Interannual and interdecadal variations in atmospheric circulation factors and rainfall in China and their relationship. *Acta Meteorol. Sin.* **2005**, *19*, 253–261.
- Shi, N.; Bueh, C. Two types of Arctic Oscillation and their associated dynamic features. *Atmos. Ocean. Sci. Lett.* **2011**, *4*, 287–292. [[CrossRef](#)]
- Kim, H.J.; Ahn, J.B. Possible impact of the autumnal North Pacific SST and November AO on the East Asian winter temperature. *J. Geophys. Res.* **2012**, *117*, D12104. [[CrossRef](#)]
- Sun, J.; Wang, H. Changes of the connection between the summer North Atlantic Oscillation and the East Asian summer rainfall. *J. Geophys. Res.* **2012**, *117*, D08110. [[CrossRef](#)]
- Cui, X.; Gao, Y.; Gong, D.; Guo, D.; Furevik, T. Teleconnection between winter Arctic Oscillation and Southeast Asian summer monsoon in the pre-industry simulation of a coupled climate model. *Atmos. Ocean. Sci. Lett.* **2013**, *6*, 349–354. [[CrossRef](#)]
- Xue, F.; Sun, D.; Zhou, T. Interdecadal and interannual variabilities of the Antarctic Oscillation simulated by CAM3. *Atmos. Ocean. Sci. Lett.* **2014**, *7*, 515–520. [[CrossRef](#)]
- Wan, J.; Li, S. Arctic Oscillation responses to black carbon aerosols emitted from major regions. *Atmos. Ocean. Sci. Lett.* **2015**, *8*, 226–232. [[CrossRef](#)]
- Zuo, J.; Ren, H.; Li, W. Contrasting Impacts of the Arctic Oscillation on Surface Air Temperature Anomalies in Southern China between Early and Mid-Late Winter. *J. Clim.* **2015**, *28*, 4015–4026. [[CrossRef](#)]
- Chen, S.; Song, L. Recent Strengthened Impact of the Winter Arctic Oscillation on the Southeast Asian Surface Air Temperature Variation. *Atmosphere* **2019**, *10*, 164. [[CrossRef](#)]
- Wang, L.; Gong, H.; Lan, X. Interdecadal variation of the Arctic Oscillation and its influence on climate. *Trans. Atmos. Sci.* **2021**, *44*, 50–60. (In Chinese) [[CrossRef](#)]
- Zhu, X.; Xu, X.; Jia, G. Asymmetrical trends of burned area between eastern and western Siberia regulated by atmospheric oscillation. *Geophys. Res. Lett.* **2021**, *48*, e2021GL096095. [[CrossRef](#)]
- Zhang, S.; Gan, T.; Bush, A.; Liu, J.; Zolina, O.; Gelfan, A. Changes of the streamflow of northern river basins of Siberia and their teleconnections to climate patterns. *Int. J. Climatol.* **2023**, *43*, 6114–6130. [[CrossRef](#)]
- Overland, J.E.; Wang, M. Large-scale atmospheric circulation changes are associated with the recent loss of Arctic sea ice. *Tellus A Dyn. Meteorol. Oceanogr.* **2010**, *62*, 1–9. [[CrossRef](#)]
- Cohen, J.L.; Furtado, J.C.; Barlow, M.A.; Alexeev, V.A.; Cherry, J.E. Arctic warming, increasing snow cover and widespread boreal winter cooling. *Environ. Res. Lett.* **2012**, *7*, 014007. [[CrossRef](#)]
- Liu, J.; Curry, J.A.; Wang, H.; Song, M.; Horton, R.M. Impact of declining Arctic Sea ice on winter snowfall. *Proc. Natl. Acad. Sci. USA* **2012**, *109*, 4074–4079. [[CrossRef](#)] [[PubMed](#)]
- Wen, M.; Yang, S.; Kumar, A.; Zhang, P. An Analysis of the Large-Scale Climate Anomalies Associated with the Snowstorms Affecting China in January 2008. *Mon. Weather Rev.* **2009**, *137*, 1111–1131. [[CrossRef](#)]
- Suo, M.; Ding, Y. The structures and evolutions of the wintertime southern branch trough in the subtropical westerlies. *Chin. J. Atmos. Sci.* **2009**, *33*, 425–442. (In Chinese)
- Zhang, Z.; Gong, D.; Hu, M.; Guo, D.; He, X.; Lei, Y. Anomalous winter temperature and precipitation events in southern China. *J. Geogr. Sci.* **2009**, *19*, 471–488. [[CrossRef](#)]

28. Mao, R.; Gong, D.; Yang, J.; Bao, J. Linkage between the Arctic Oscillation and winter extreme precipitation over central-southern China. *Clim. Res.* **2011**, *50*, 187–201. [[CrossRef](#)]
29. Gu, W.; Li, C.; Li, W.; Zhou, W.; Chan, J.C.L. Interdecadal unstationary relationship between NAO and east China's summer precipitation patterns. *Geophys. Res. Lett.* **2009**, *36*, L13702. [[CrossRef](#)]
30. Gong, D.; Wang, S. Influence of Arctic Oscillation on winter climate over China. *J. Geogr. Sci.* **2003**, *13*, 208–216. [[CrossRef](#)]
31. Xu, H.; Li, J.; Feng, J.; Mao, J. The asymmetric relationship between the winter NAO and the precipitation in Southwest China. *Acta Meteorol. Sin.* **2012**, *70*, 1276–1291. (In Chinese) [[CrossRef](#)]
32. Yang, S.; Lau, K.M.; Yoo, S.H.; Kinter, J.L.; Miyakoda, K.; Ho, C.H. Upstream Subtropical Signals Preceding the Asian Summer Monsoon Circulation. *J. Clim.* **2004**, *17*, 4213–4229. [[CrossRef](#)]
33. Wu, B.; Wang, J. Possible impacts of winter Arctic Oscillation on Siberian high, the East Asian winter monsoon and sea-ice extent. *Adv. Atmos. Sci.* **2002**, *19*, 297–320. [[CrossRef](#)]
34. Chen, S.; Chen, W. Distinctive impact of spring AO on the succedent winter El Niño event: Sensitivity to AO's North Pacific component. *Clim. Dyn.* **2022**, *58*, 235–255. [[CrossRef](#)]
35. Cai, Q.; Wang, J.; Beletsky, D.; Overland, J.; Ikeda, M.; Wan, L. Accelerated decline of summer Arctic sea ice during 1850–2017 and the amplified Arctic warming during the recent decades. *Environ. Res. Lett.* **2021**, *16*, 034015. [[CrossRef](#)]
36. Cai, Q.; Beletsky, D.; Wang, J.; Lei, R. Interannual and Decadal Variability of Arctic Summer Sea Ice Associated with Atmospheric Teleconnection Patterns during 1850–2017. *J. Clim.* **2021**, *34*, 9931–9955. [[CrossRef](#)]
37. Papritz, L. Arctic Lower-Tropospheric Warm and Cold Extremes: Horizontal and Vertical Transport, Diabatic Processes, and Linkage to Synoptic Circulation Features. *J. Clim.* **2020**, *33*, 993–1016. [[CrossRef](#)]
38. Chen, W.; Zhou, Q. Modulation of the Arctic Oscillation and the East Asian winter climate relationships by the 11-year solar cycle. *Adv. Atmos. Sci.* **2012**, *29*, 217–226. [[CrossRef](#)]
39. Li, F.; Wang, H.; Gao, Y. On the Strengthened Relationship between the East Asian Winter Monsoon and Arctic Oscillation: A Comparison of 1950–70 and 1983–2012. *J. Clim.* **2014**, *27*, 5075–5091. [[CrossRef](#)]
40. Li, F.; Wang, H.; Liu, J. The strengthening relationship between Arctic Oscillation and ENSO after the mid-1990s. *Int. J. Climatol.* **2014**, *34*, 2515–2521. [[CrossRef](#)]
41. Huang, W.; Wang, B.; Wright, J.S.; Chen, R. On the Non-Stationary Relationship between the Siberian High and Arctic Oscillation. *PLoS ONE* **2016**, *11*, e0158122. [[CrossRef](#)] [[PubMed](#)]
42. Liu, Y.; He, S.; Li, F.; Wang, H.; Zhu, Y. Interdecadal change between the Arctic Oscillation and East Asian climate during 1900–2015 winters. *Int. J. Climatol.* **2017**, *37*, 4791–4802. [[CrossRef](#)]
43. Gong, H.; Wang, L.; Chen, W.; Nath, D. Multidecadal Fluctuation of the Wintertime Arctic Oscillation Pattern and Its Implication. *J. Clim.* **2018**, *31*, 5595–5608. [[CrossRef](#)]
44. Qiao, S.; Hu, P.; Feng, T.; Cheng, J.; Han, Z.; Gong, Z.; Zhi, R.; Feng, G. Enhancement of the relationship between the winter Arctic oscillation and the following summer circulation anomalies over central East Asia since the early 1990s. *Clim. Dyn.* **2018**, *50*, 3485–3503. [[CrossRef](#)]
45. Gong, H.; Wang, L.; Chen, W. Multidecadal Changes in the Influence of the Arctic Oscillation on the East Asian Surface Air Temperature in Boreal Winter. *Atmosphere* **2019**, *10*, 757. [[CrossRef](#)]
46. Shen, B.; Lin, Z.; Lu, R.; Lian, Y. Circulation anomalies associated with interannual variation of early- and late-summer precipitation in Northeast China. *Sci China Earth Sci.* **2011**, *54*, 1095–1104. [[CrossRef](#)]
47. Zhou, J.; Zhao, J.; He, W.; Gong, Z. Spatiotemporal characteristics and water budget of water cycle elements in different seasons in northeast China. *Chin. Phys. B* **2015**, *24*, 049203. [[CrossRef](#)]
48. Kistler, R.; Kalnay, E.; Collins, W.; Saha, S.; White, G.; Woollen, J.; Chelliah, M.; Ebisuzaki, W.; Kanamitsu, M.; Kousky, V.; et al. The NCEP–NCAR 50-Year Reanalysis: Monthly means CD-ROM and documentation. *Bull. Am. Meteor. Soc.* **2001**, *82*, 247–268. [[CrossRef](#)]
49. Compo, G.P.; Whitaker, J.S.; Sardeshmukh, P.D. Feasibility of a 100-Year Reanalysis Using Only Surface Pressure Data. *Bull. Am. Meteorol. Soc.* **2006**, *87*, 175–190. [[CrossRef](#)]
50. Schneider, U.; Becker, A.; Finger, P.; Meyer-Christoffer, A.; Ziese, M.; Rudolf, B. GPCC's new land surface precipitation climatology based on quality-controlled in situ data and its role in quantifying the global water cycle. *Theor. Appl. Climatol.* **2014**, *115*, 15–40. [[CrossRef](#)]
51. Matsuura, K.; Willmott, C.J. *Terrestrial Air Temperature: 1900–2008 Gridded Monthly Time Series (Version 4.01)*; University of Delaware Department of Geography Center: Newark, DE, USA, 2009. Available online: https://www.esrl.noaa.gov/psd/data/gridded/data.UDel_AirT_Precip.html (accessed on 24 December 2022).
52. Huang, B.; Thorne, P.W.; Banzon, V.F.; Boyer, T.; Chepurin, G.; Lawrimore, J.H.; Menne, M.J.; Smith, T.M.; Vose, R.S.; Zhang, H.-M. Extended reconstructed sea surface temperature, version 5 (ERSSTv5): Upgrades, validations, and intercomparisons. *J. Clim.* **2017**, *30*, 8179–8205. [[CrossRef](#)]
53. North, G.R.; Bell, T.L.; Cahalan, R.F.; Moeng, F.J. Sampling Errors in the Estimation of Empirical Orthogonal Functions. *Mon. Weather Rev.* **1982**, *110*, 699–706. [[CrossRef](#)]
54. Takaya, K.; Nakamura, H. A Formulation of a Phase-Independent Wave-Activity Flux for Stationary and Migratory Quasi-geostrophic Eddies on a Zonally Varying Basic Flow. *J. Atmos. Sci.* **2001**, *58*, 608–627. [[CrossRef](#)]

55. Shaman, J. The Seasonal Effects of ENSO on European Precipitation: Observational Analysis. *J. Clim.* **2014**, *27*, 6423–6438. [[CrossRef](#)]
56. Zhou, Y.; Wu, Z. Possible impacts of mega-El Niño/Southern Oscillation and Atlantic Multidecadal Oscillation on Eurasian heatwave frequency variability. *Q. J. R. Meteorol. Soc.* **2016**, *142*, 1647–1661. [[CrossRef](#)]
57. Nuncio, M.; Chatterjee, S.; Satheesan, K.; Chenoli, S.N.; Subeesh, M.P. Temperature and precipitation during winter in NyÅlesund, Svalbard and possible tropical linkages. *Tellus A Dyn. Meteorol. Oceanogr.* **2020**, *72*, 1–15. [[CrossRef](#)]
58. Yamagata, T.; Behera, S.K.; Luo, J.; Masson, S.; Jury, M.R.; Rao, S.A. Coupled Ocean-Atmosphere Variability in the Tropical Indian Ocean. *Earth's Clim. Ocean. Atmos. Interact. Geophys. Monogr.* **2004**, *147*, 189–211. [[CrossRef](#)]
59. Karagiannidis, A.F.; Bloutsos, A.A.; Maheras, P.; Sachsamanoglou, C. Some statistical characteristics of precipitation in Europe. *Theor. Appl. Climatol.* **2008**, *91*, 193–204. [[CrossRef](#)]
60. Wang, J.; Gui, S.; Ma, A.; Yang, R.; Zhang, Q. Interdecadal Variability of Summer Precipitation Efficiency in East Asia. *Adv. Meteorol.* **2019**, *2019*, 3563024. [[CrossRef](#)]
61. Wen, N.; Liu, Z.; Li, L. Direct ENSO impact on East Asian summer precipitation in the developing summer. *Clim. Dyn.* **2019**, *52*, 6799–6815. [[CrossRef](#)]
62. Maialen, M.D.; Jorge, L.P.; Belén, R.F.; Losada, T. The stationarity of the ENSO teleconnection in European summer rainfall. *Clim. Dyn.* **2023**, *61*, 489–506. [[CrossRef](#)]
63. Yan, L.; Li, G. Change in the Relationship between the Southern Subtropical Dipole Modes and the Southern Annular Mode in the Mid-1980s. *J. Clim.* **2015**, *28*, 9235–9249. [[CrossRef](#)]
64. Hao, S.; Li, J.; Mao, J. Interannual relationship between summer North Atlantic Oscillation and subsequent November precipitation anomalies over Yunnan in Southwest China. *J. Meteor. Res.* **2022**, *36*, 718–732. [[CrossRef](#)]
65. Li, C. *Introduction to Climate Dynamics*, 2nd ed.; China Meteorological Press: Beijing, China, 2000. (In Chinese)
66. Hoskins, B.J.; Ambrizzi, T. Rossby wave propagation on a realistic longitudinally varying flow. *J. Atmos. Sci.* **1993**, *50*, 1661–1671. [[CrossRef](#)]
67. Takaya, K.; Nakamura, H. A formulation of a wave-activity flux for stationary Rossby waves on a zonally varying basic flow. *Geophys. Res. Lett.* **1997**, *24*, 2985–2988. [[CrossRef](#)]
68. Miao, R.; Wen, M.; Zhang, R.; Li, L. The influence of wave trains in mid-high latitudes on persistent heavy rain during the first rainy season over South China. *Clim. Dyn.* **2019**, *53*, 2949–2968. [[CrossRef](#)]
69. Deng, K.; Yang, S.; Ting, M.; Lin, A.; Wang, Z. An intensified mode of variability modulating the summer heat waves in eastern Europe and northern China. *Geophys. Res. Lett.* **2018**, *45*, 361–369. [[CrossRef](#)]
70. Chen, S.; Wu, R.; Chen, W.; Hu, K.; Yu, B. Structure and dynamics of a springtime atmospheric wave train over the North Atlantic and Eurasia. *Clim. Dyn.* **2020**, *54*, 5111–5126. [[CrossRef](#)]
71. Watanabe, M. Asian Jet Waveguide and a Downstream Extension of the North Atlantic Oscillation. *J. Clim.* **2004**, *17*, 4674–4691. [[CrossRef](#)]
72. Ding, Q.; Wang, B. Circumglobal Teleconnection in the Northern Hemisphere Summer. *J. Clim.* **2005**, *18*, 3483–3505. [[CrossRef](#)]
73. Sung, M.K.; Kwon, W.T.; Baek, H.J.; Boo, K.O.; Lim, G.H.; Kug, J.S. A possible impact of the North Atlantic Oscillation on the east Asian summer monsoon precipitation. *Geophys. Res. Lett.* **2006**, *33*, L21713. [[CrossRef](#)]
74. Linderholm, H.W.; Ou, T.; Jeong, J.H.; Folland, C.K.; Gong, D.; Liu, H.; Liu, Y.; Chen, D. Interannual teleconnections between the summer North Atlantic Oscillation and the East Asian summer monsoon. *J. Geophys. Res.* **2011**, *116*, D13107. [[CrossRef](#)]
75. Linderholm, H.W.; Seim, A.; Ou, T.; Jeong, J.H.; Liu, Y.; Wang, X.; Bao, G.; Folland, C.K. Exploring teleconnections between the summer NAO (SNAO) and climate in East Asia over the last four centuries—A tree-ring perspective. *Dendrochronologia* **2013**, *31*, 297–310. [[CrossRef](#)]
76. Bollasina, M.A.; Messori, G. On the link between the subseasonal evolution of the North Atlantic Oscillation and East Asian climate. *Clim. Dyn.* **2018**, *51*, 3537–3557. [[CrossRef](#)]
77. Wang, Z.; Yang, Z.; Lau, N.C.; Duan, A. Teleconnection between Summer NAO and East China Rainfall Variations: A Bridge Effect of the Tibetan Plateau. *J. Clim.* **2018**, *31*, 6433–6444. [[CrossRef](#)]
78. Wu, X.; Hao, Z.; Hao, F.; Zhang, X.; Singh, V.P.; Sun, C. Influence of large-scale circulation patterns on compound dry and hot events in China. *J. Geophys. Res. Atmos.* **2021**, *126*, e2020JD033918. [[CrossRef](#)]
79. Lu, R.Y.; Oh, J.H.; Kim, B.J. A teleconnection pattern in upper-level meridional wind over the North African and Eurasian continent in summer. *Tellus A Dyn. Meteorol. Oceanogr.* **2002**, *54*, 44–55. [[CrossRef](#)]
80. Enomoto, T.; Hoskins, B.J.; Matsuda, Y. The formation mechanism of the Bonin high in August. *Q. J. R. Meteorol. Soc.* **2003**, *129*, 157–178. [[CrossRef](#)]
81. Jin, D.; Guan, Z. Summer Rainfall Seesaw between Hetao and the Middle and Lower Reaches of the Yangtze River and Its Relationship with the North Atlantic Oscillation. *J. Clim.* **2017**, *30*, 6629–6643. [[CrossRef](#)]
82. Zhou, F.; Zhang, R.; Han, J. Relationship between the Circumglobal Teleconnection and Silk Road Pattern over Eurasian continent. *Sci. Bull.* **2019**, *64*, 374–376. [[CrossRef](#)]
83. Yan, M.; Liu, J. Physical processes of cooling and mega-drought during the 4.2 ka BP event: Results from TraCE-21ka simulations. *Clim. Past* **2019**, *15*, 265–277. [[CrossRef](#)]
84. Shang, W.; Duan, K.; Li, S.; Ren, X.; Haung, B. Simulation of the dipole pattern of summer precipitation over the Tibetan Plateau by CMIP6 models. *Environ. Res. Lett.* **2021**, *16*, 014047. [[CrossRef](#)]

85. Hong, X.; Lu, R.; Chen, S.; Li, S. The Relationship between the North Atlantic Oscillation and the Silk Road Pattern in Summer. *J. Clim.* **2022**, *35*, 6691–6702. [[CrossRef](#)]
86. Saeed, S.; Müller, W.A.; Hagemann, S.; Jacob, D. Circumglobal wave train and the summer monsoon over northwestern India and Pakistan: The explicit role of the surface heat low. *Clim. Dyn.* **2011**, *37*, 1045–1060. [[CrossRef](#)]
87. Wu, B.; Lin, J.; Zhou, T. Interdecadal circumglobal teleconnection pattern during boreal summer. *Atmos. Sci. Lett.* **2016**, *17*, 446–452. [[CrossRef](#)]
88. Sun, X.; Li, S.; Hong, X.; Lu, R. Simulated influence of the Atlantic Multidecadal Oscillation on summer Eurasian nonuniform warming since the mid-1990s. *Adv. Atmos. Sci.* **2019**, *36*, 811–822. [[CrossRef](#)]
89. Du, Y.; Zhang, J.; Zhao, S.; Chen, H. Impact of the eastward shift in the negative—Phase NAO on extreme drought over northern China in summer. *J. Geophys. Res. Atmos.* **2020**, *125*, e2019JD032019. [[CrossRef](#)]
90. Limpasuvan, V.; Hartmann, D.L. Wave-Maintained Annular Modes of Climate Variability. *J. Clim.* **2000**, *13*, 4414–4429. [[CrossRef](#)]
91. Saunders, M.A.; Qian, B. Seasonal predictability of the winter NAO from north Atlantic sea surface temperatures. *Geophys. Res. Lett.* **2002**, *29*, 2049. [[CrossRef](#)]
92. Rao, J.; Ren, R. Varying stratospheric responses to tropical Atlantic SST forcing from early to late winter. *Clim. Dyn.* **2018**, *51*, 2079–2096. [[CrossRef](#)]
93. Vihma, T. Effects of Arctic Sea Ice Decline on Weather and Climate: A Review. *Surv. Geophys.* **2014**, *35*, 1175–1214. [[CrossRef](#)]
94. Liu, Y.; Chen, H.; Wang, H.; Sun, J.; Li, H.; Qiu, Y. Modulation of the Kara Sea Ice Variation on the Ice Freeze-Up Time in Lake Qinghai. *J. Clim.* **2019**, *32*, 2553–2568. [[CrossRef](#)]
95. Li, Y.; Zhang, L.; Gan, B.; Wang, H.; Li, X.; Wu, L. Observed contribution of Barents-Kara sea ice loss to Warm Arctic-Cold Eurasia anomalies by submonthly processes in winter. *Environ. Res. Lett.* **2023**, *18*, 034019. [[CrossRef](#)]
96. Tabari, H. Climate change impact on flood and extreme precipitation increases with water availability. *Sci. Rep.* **2020**, *10*, 13768. [[CrossRef](#)]
97. Zhang, W.; Furtado, K.; Wu, P.; Zhou, T.; Chadwick, R.; Marzin, C.; Rostron, J.; Sexton, D. Increasing precipitation variability on daily-to-multiyear time scales in a warmer world. *Sci. Adv.* **2021**, *7*, eabf8021. [[CrossRef](#)] [[PubMed](#)]
98. Zhao, J.; Cao, Y.; Shi, J. Spatial variation of the Arctic Oscillation and its long-term change. *Tellus A Dyn. Meteorol. Oceanogr.* **2010**, *62*, 661–672. [[CrossRef](#)]

Disclaimer/Publisher’s Note: The statements, opinions and data contained in all publications are solely those of the individual author(s) and contributor(s) and not of MDPI and/or the editor(s). MDPI and/or the editor(s) disclaim responsibility for any injury to people or property resulting from any ideas, methods, instructions or products referred to in the content.